CLAS12 GPD program

S. STEPANYAN (JLAB)

LEPTON INTERACTIONS WITH NUCLEONS AND NUCLEI

17TH WORKSHOP, JUNE 22 TO 27, 2025

MARCIANA MARINA (ISOLA D'ELBA), ITALY

OFFICE OF SCIENCE

Jefferson Lab
Thomas Jefferson National Accelerator Facility

Outline

- 3D structure of the nucleon and GPD framework
- Experimental observables and GPDs
- Deeply Virtual Exclusive Reactions with CLAS12
- Opportunities with high luminosity CLAS12
- Summary

e-Scattering for Nucleon Tomography

Elastic and DIS project out two orthogonal views.

DIS Parton Distribution Functions

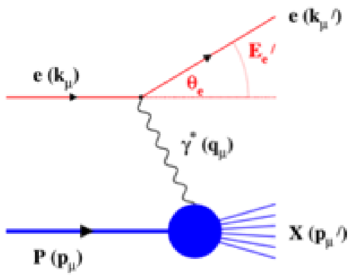

No information on the spatial location of the constituents

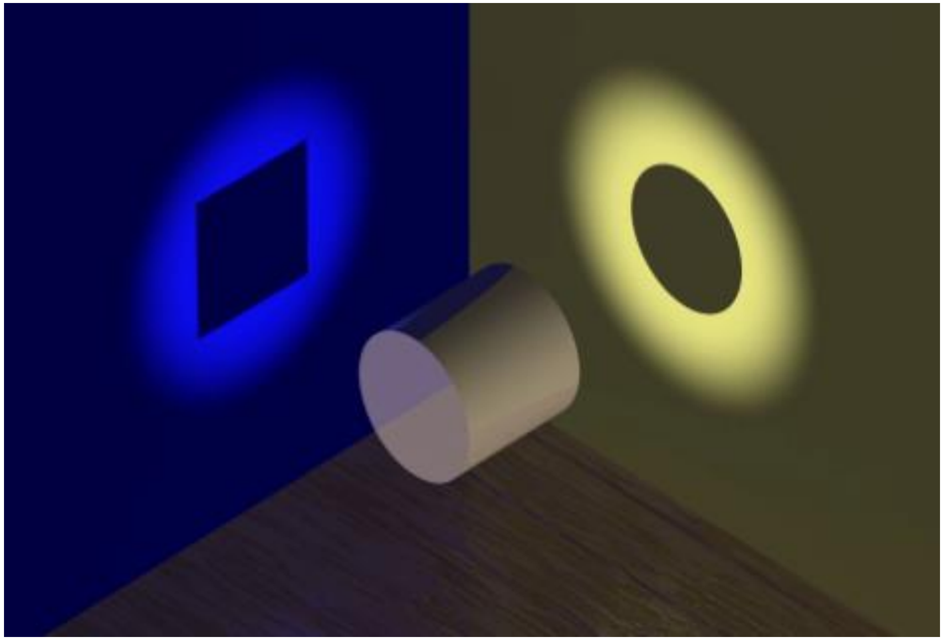

Elastic Form Factors

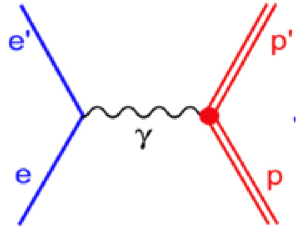

No information about the underlying dynamics of the system

Developed in the late 90s, the formalism of Generalized Parton Distributions (GPDs) has laid the path towards 3-D imaging of the nucleon's partonic structure and determination of nucleons' fundamental properties using deep exclusive processes.

GPD framework

- GPDs are the probability amplitudes for finding a particular partonic configuration inside the nucleon and provide access to the transverse spatial and longitudinal momentum distributions of partons.
- The factorization theorem provides the basis for accessing GPDs experimentally through deeply virtual exclusive processes (DVCS, TCS, DVMP)

At leading-twist, there are four chiral-even GPDs:
H and $\widetilde{H}$, nucleon helicity conserving
E and $\widetilde{E}$, nucleon helicity flip

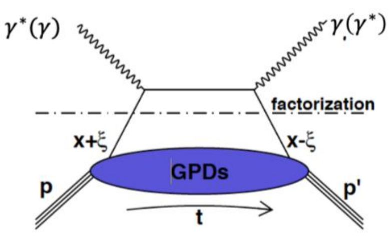

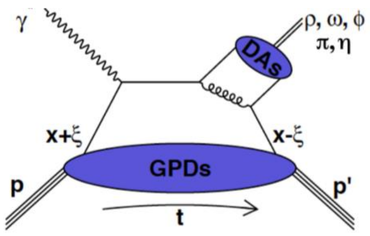

In the forward limit ($\xi \to 0, t \to 0$)
H and $\widetilde{H}$ GPD reduce to parton PDFs

$$H^a(x,0,0) = a(x) - \bar{a}(x)$$

$$\widetilde{H}^a(x,0,0) = \Delta a(x) - \Delta\bar{a}(x)$$

The first moments of quark GPDs are related to the Dirac, Pauli, axial, and pseudoscalar form factors

$$\int_{-1}^{1} dx\, H^q(x,\xi,t) = F_1^q(t) \qquad \int_{-1}^{1} \widetilde{H}^q(x,\xi,t) = g_A^q(t)$$

$$\int_{-1}^{1} dx\, E^q(x,\xi,t) = F_2^q(t) \qquad \int_{-1}^{1} \widetilde{E}^q(x,\xi,t) = h_A^q(t)$$

GPDs and FFs of the QCD EMT

$$\langle P'|T^{\mu\nu}_{q,g}|P\rangle = \bar{u}\left(P'\right)\left[A_{q,g}(t)\frac{P^\mu P^\nu}{M} + C_{q,g}(t)\frac{\left(\Delta^\mu\Delta^\nu - g^{\mu\nu}\Delta^2\right)}{M} + \bar{C}_{q,g}(t)g^{\mu\nu}M\right.$$
$$\left. + \left[A_{q,g}(t) + B_{q,g}(t)\right]\frac{P^{\{\mu}i\sigma^{\nu\}\Delta}}{4M} + D_{q,g}(t)\frac{P^{\{\mu}i\sigma^{\nu\}\Delta}}{4M}\right]u(P).$$

Three of the GFFs, *A*, *B*, and *C,* can be derived from the 2nd Mellin moment of leading-twist GPDs *E* and *H:*

$$\int_{-1}^{1} dx\, x\, H^{q,g}(x,\xi,t) = A_{q,g}(t) + \xi^2 C_{q,g}(t) \qquad \int_{-1}^{1} dx\, x\, E^{q,g}(x,\xi,t) = A_{q,g}(t) - \xi^2 C_{q,g}(t)$$

A, *B*, and *C,* define the mass distribution in the nucleon and its spin carried by quarks and gluons:

$$G_m(t) = \left[M A_{q+g}(t) + B_{q+g}(t)\frac{t}{4M} - C_{q+g}(t)\frac{t}{M}\right]$$

$$\langle r^2\rangle_m = 6 \left| \frac{dG_m(t)/M}{dt} \right|_{t=0}.$$

$$J_{q,g} = \frac{1}{2}\left[A_{q,g} + B_{q,g}\right]$$

Ji, Phys. Rev. Lett. 77 / Phys. Rev. D 55, 1997.

$$= \frac{1}{2}\int_{-1}^{1} dx\, x\left(H^{q,g}(x,\xi,0) + E^{q,g}(x,\xi,0)\right)$$

The GFFs $C(t)$, and $\bar{C}(t)$ characterize the shear forces, $s(r)$, and the pressure, $p(r)$, distributions inside the nucleon.

V. Burkert et al., Reviews of Modern Physics, volume 95, 2023

From experimental observables to GPDs

- The process amplitude depends on CFFs, $\mathcal{T} \sim \mathcal{F}(\xi, t)$, where GPDs ($F$) enter via convolution integrals:

$$\mathcal{F}^{\pm}(\xi, t) = \int_{-1}^{1} dx \left(\frac{1}{\xi - x + i\varepsilon} \mp \frac{1}{\xi + x + i\varepsilon} \right) F(x, \xi, t)$$ at lowest order in α_s

- The imaginary part of CFFs is accessed via single spin asymmetries and probes GPDs at $x = \pm\xi$: $Im\mathcal{F}(\xi, t) = i\pi \sum_a [F^a(\xi, \xi, t) - F^a(-\xi, \xi, t)]$

- Real part: accessed via cross sections, charge and double spin asymmetries; involves integrals over x: $Re\mathcal{F}(\xi, t) = P \int_{-1}^{1} dx \left(\frac{1}{\xi - x} \pm \frac{1}{\xi + x} \right) \sum_a [F^a(x, \xi, t) \mp F^a(-x, \xi, t)]$

- Inferring GPDs from experimental observables is a multistep process:
  - Fit CFFs to experimental observables
  - Model GPDs using parametrizations (Double Distributions, Regge models, neural networks)
  - Global analysis combining multiple channels and experiments

- Deconvolution challenges: limited kinematic coverage, theoretical uncertainties (higher twists, NLO corrections), and model ambiguities (different GPD parametrizations can fit existing data).

  The key limitation on the experimental side is that current measurements access only two of the three GPD variables (x, ξ, t), since the variable x is integrated out in the convolution integral.

- More data for different reactions across a wide kinematic range is needed.

CLAS12 in Hall-B at JLAB

Designed luminosity $10^{35}\mathrm{cm}^{-2}\mathrm{sec}^{-1}$

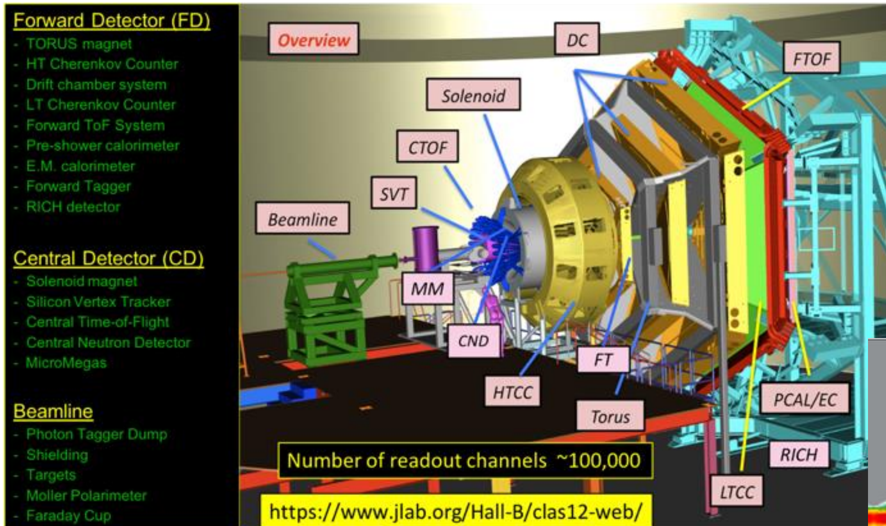

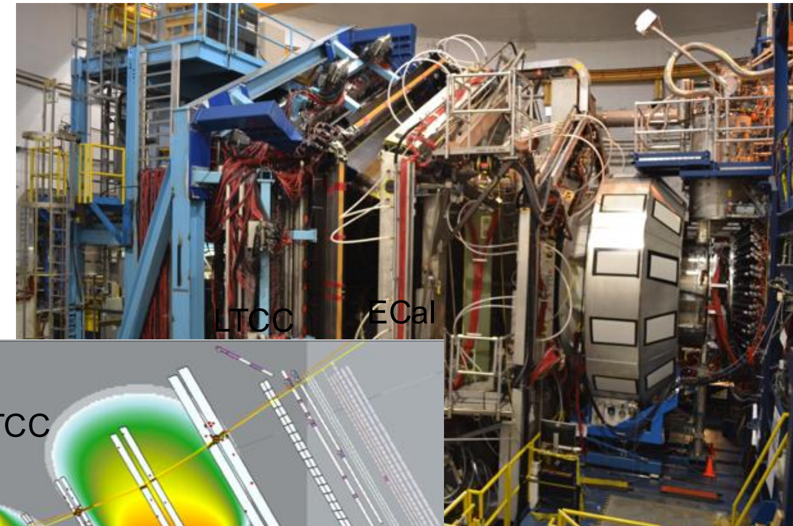

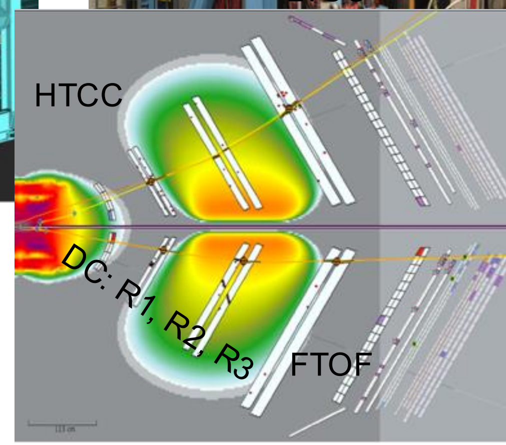

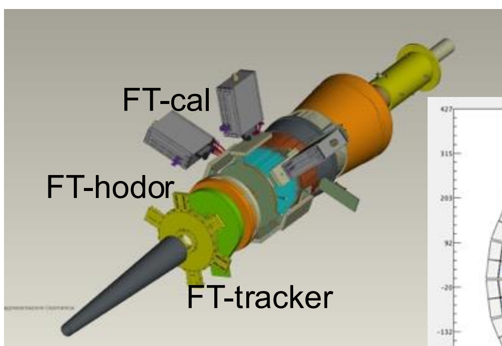

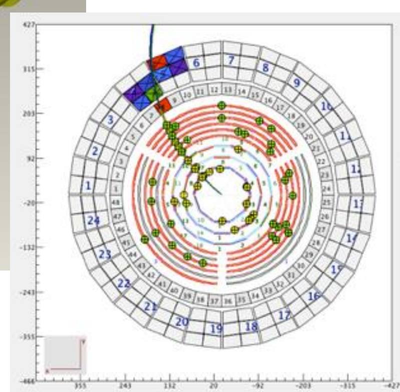

Physics targets:
- LH_2, LD_2, LHe, LAr, D, ^{4}He
- ^{12}C to ^{208}Pb
- Polarized NH_3, ND_3

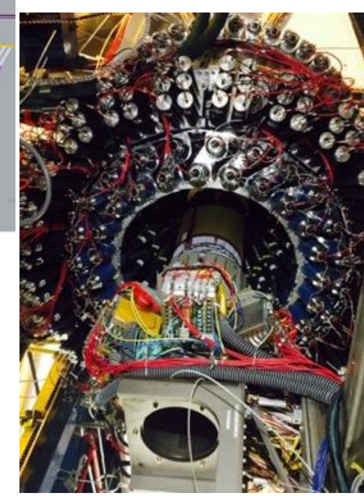

CLAS12 GPD program

- The subject of nuclear femtography is a central focus of the CLAS12 science program – 500 PAC-approved days of beam running.
- Planned studies, built on the successful GPD program at 6 GeV with CLAS, will provide numerous data points on cross sections, beam, target (L/T), and double-spin asymmetries.
- Experiments are already underway, using unpolarized and polarized targets with up to 11 GeV longitudinally polarized electron beams.

Proposal	Physics	Contact	Rating	Days	Group	New equipment	Energy	Run Group	Target	Complete
E12-06-108	Hard exclusive electro-production of π^0, η	Stoler	B	80	139	RICH (1 sector) Forward tagger			liquid H_2	
E12-06-108A	Exclusive N*->KY Studies with CLAS12	Carman		(60)						
E12-06-108B	Transition Form Factor of the η' Meson with CLAS12	Kunkel		(80)						
E12-06-112	Proton's quark dynamics in SIDIS pion production	Avakian	A	60						
E12-06-112A	Semi-inclusive Λ productiuon in target fragmentation region	Mirazita		(60)						
E12-06-112B	Colinear nucleon structure at twist-3	Pisano		(60)						
E12-06-119(a)	Deeply Virtual Compton Scattering	Sabatie	A	80						
E12-09-003	Excitation of nucleon resonances at high Q^2	Gothe	B+	40						
E12-11-005	Hadron spectroscopy with forward tagger	Battaglieri	A-	119						
E12-11-005A	Photoproduction of the very strangest baryon	Guo		(120)						
E12-12-001	Timelike Compton Scatt. & J/ψ production in e+e-	Nadel-Turonski	A-	120						
E12-12-001A	Near Threshold J/ψ photoproduction and study of LHCb pentquarks	Stepanyan		(120)						
E12-12-007	Exclusive φ meson electroproduction with CLAS12	Stoler, Weiss	B+	60						
E12-07-104	Neutron magnetic form factor	Gilfoyle	A-	30	90					
E12-09-007(a)	Study of partonic distributions in SIDIS kaon production	Hafidi	A-	30						
E12-09-008	Boer-Mulders asymmetry in K SIDIS w/ H and D targets	Contalbrigo	A-	56						
E12-09-008A	Hadron production in target fragmentation region	Mirazita		(60)						43%
E12-09-008B	Colinear nucleon structuer at twist-3	Pisano		(60)						
E12-11-003	DVCS on neutron target	Niccolai	A	90						
E12-11-003A	In medium structure functions, SRC, and the EMC effect	Hen		(90)						

Proposal	Physics	Contact	Rating	Days	Group	Equipment	Energy (GeV)	Group	Target	Complete
E12-06-109	Longitudinal Spin Structure of the Nucleon	Kuhn	A	80	~~185~~ 120	Longitudinally Polarized target RICH (1 sector) Forward tagger	11	**C** S. Kuhn	NH_3 ND_3	
E12-06-109A	DVCS on the neutron with polarized deuterium target	Niccolai		(60)						
E12-06- 119(b)	DVCS on longitudinally polarized proton target	Sabatie	A	120						
E12-07-107	Spin-Orbit Correl. with Longitudinally polarized target	Avakian	A-	103						
E12-09-007(b)	Study of partonic distributions using SIDIS K production	Hafidi	A-	80						
E12-09-009	Spin-Orbit correlations in K production w/ pol. targets	Avakian	B+	103						
E12-06-106	Color transparency in exclusive vector meson production	Hafidi(El Fassi)	B+	~~60~~ 30	30		11	**D**		
E12-06-106A	Nuclear TMDs in CLAS12	Dupre		(30)						
E12-06-117	Quark propagation and hadron formation	Brooks	A-	60	60		11	**E**	Nuclear	
E12-06-113	Free Neutron structure at large x	Bueltman	A	42	42	Radial TPC	11	**F**	Gas D_2	100%
E12-14-001	EMC effect in spin structure functions	Brooks	B+	55	55	Pol. target, Li	11	**G**	6LiH/7LiD	
C12-11-111	SIDIS on transverse polarized target	Contalbrigo	A	110	110	Transversely polarized target	11	**H**	HD	
C12-12-009	Transversity w/ di-hadron on transvere target	Avakian	A	110						
C12-12-010	DVCS with transverse polarized target in CLAS12	Elouadrhriri	A	110						

Proposal	Physics	Contact	Rating	Days app.	Group	Equipment	Energy (GeV)	Group	Target	Completed
E12-16-010	A search for Hybrid Baryons in Hall B with CLAS12	D'Angelo	A-	100	**100**	Forward Tagger	6.6, 8.8	**K** Confinement & Strong QCD	**LH2**	**12%**
E12-16-010A	Nucleon Resonances in exc. KY electroproduction	Carman	A-	(100)						
E12-16-010B	DVCS with CLAS12 at 6.6 and 8.8 GeV	Elouadrhiri	A-	(100)						
E12-17-012	Partonic Structure of Light Nuclei	Meziani	A-	55	**55**	ALERT detector	11	**L**	**High pressure gas H, D, 4He**	
E12-17-012A	Tagged EMC measurements on Light Nuclei	Dupre								
E12-17-012B	Spectator-Tagged DVCS on Light Nuclei	Armstrong								
E12-17-012C	Other Physics Opportunities with ALERT	Hafidi								

Proton DVCS: BSA

G. Christiaens, et al., CLAS Collaboration, Phys. Rev. Lett. 130, 211902 (2023).

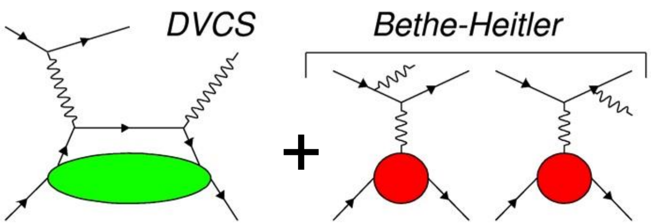

$$\sigma(ep \to e'p'\gamma) = \sigma_{BH} + \sigma_{DVCS} + \sigma_{INT}$$

$$A_{LU} = \frac{1}{P_B}\frac{N^+ - N^-}{N^+ + N^-}$$

$$A_{\mathrm{LU}}(\phi) \sim \frac{s^{\mathcal{I}}_{1,\mathrm{unp}} \sin\phi}{c^{\mathrm{BH}}_{0,\mathrm{unp}} + (c^{\mathrm{BH}}_{1,\mathrm{unp}} + c^{\mathcal{I}}_{1,\mathrm{unp}} + \cdots)\cos\phi \cdots}$$

$$s^{\mathcal{I}}_{1,\mathrm{unp}} \propto \Im\mathrm{m}\left[F_1\mathcal{H} + \xi(F_1+F_2)\tilde{\mathcal{H}} - \frac{t}{4M^2}F_2\mathcal{E}\right]$$

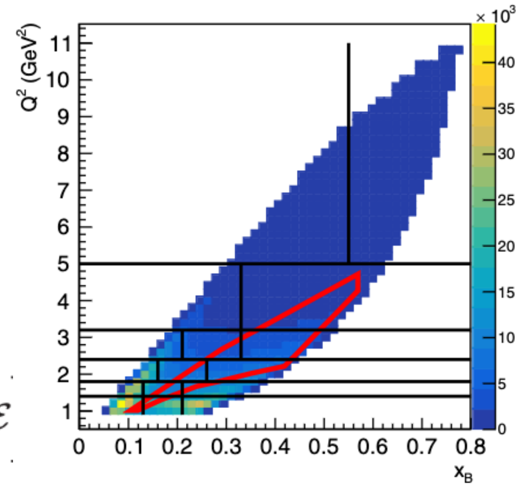

The kinematic region overlaps with previously published CLAS data. KM15 parameters and AAN training use the available world dataset on DVCS.

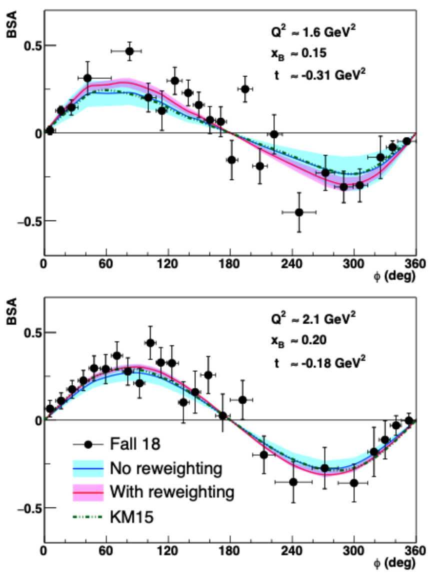

- Kinematic bins that are accessible only with a ~10 GeV electron beam.
- KM15, VGG, and GK models provide a reasonable description of the data.

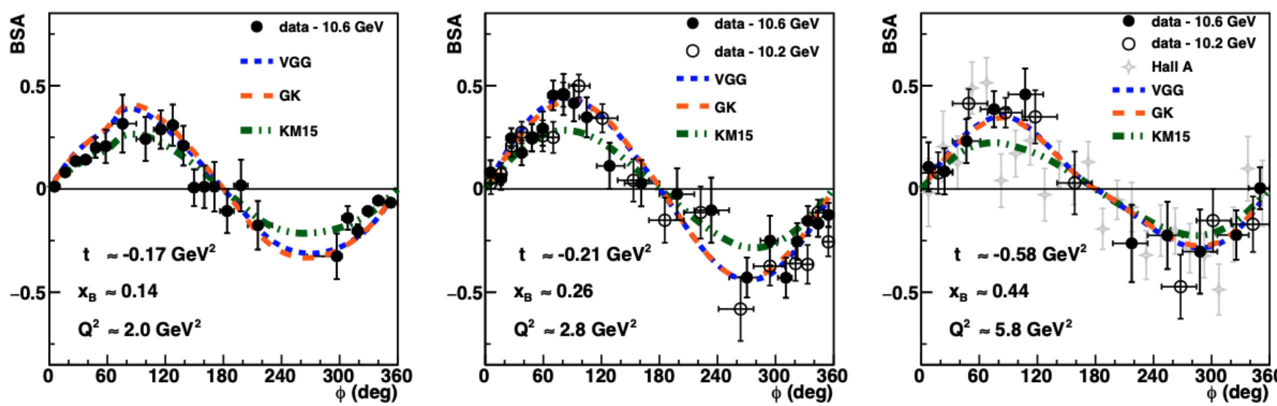

Neutron DVCS

A. Hobart et al., CALS collaboration, Phys. Rev. Lett. 133, 211903 (2024).

The first measurement of BSA for *n*DVCS in a fully exclusive reaction using deuterium as a neutron target.

$$\sigma(ed \rightarrow e'n\gamma(p)) = \sigma_{BH} + \sigma_{DVCS} + \sigma_{INT}$$

$$A_{LU} \propto \sin\phi\ \Im m\left(F_1\mathcal{H} + \xi(F_1+F_2)\tilde{\mathcal{H}} - \frac{t}{4M^2}\mathcal{E}\right)$$

BSA is sensitive to the CFF E and provides access to the GPD E, one of the ingredients in Ji's spin sum rule.

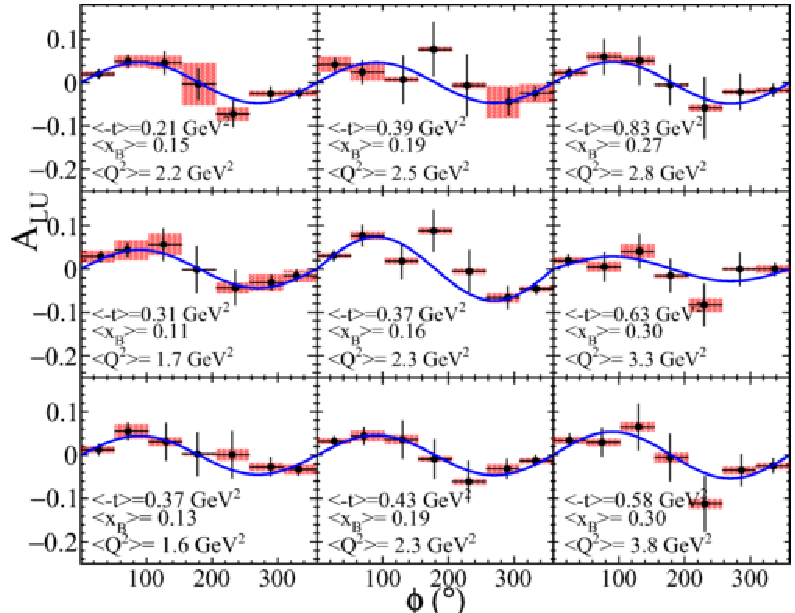

Extraction of the ***u*** and ***d*** quark contributions to $\Im m\mathcal{H}$ and $\Im m\mathcal{E}$

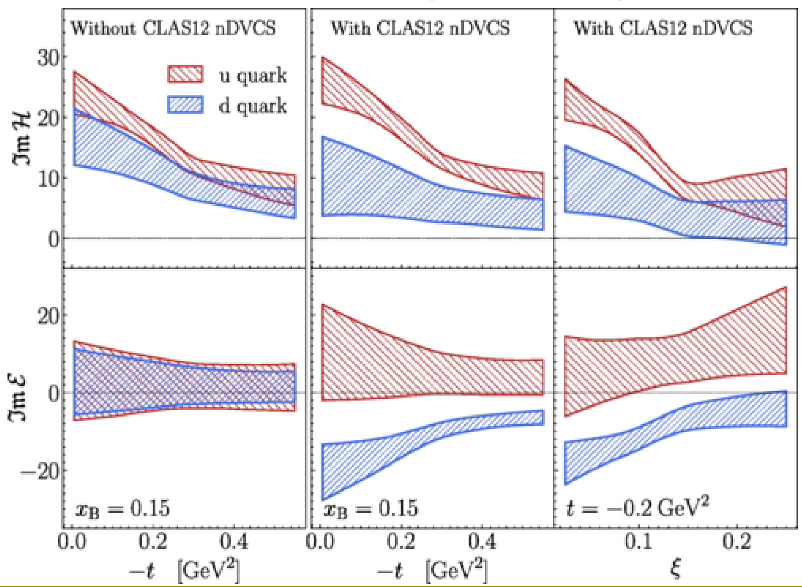

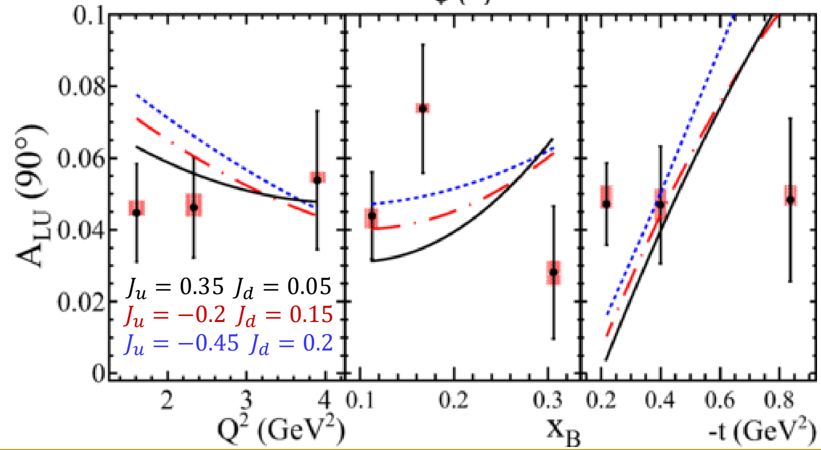

DVCS with longitudinally polarized NH_3 and ND_3

Credit to S.Niccolai, S. Polcher Rafael,

Observables $\boldsymbol{A_{UL}}$ for the imaginary part of the CFF $\mathcal{H}$ and $\widetilde{\mathcal{H}}$, and $\boldsymbol{A_{LL}}$ to access to the real part.

$$A_{\mathrm{UL}}(\phi) \sim \frac{s^{\mathcal{I}}_{1,\mathrm{LP}} \sin\phi}{c^{\mathrm{BH}}_{0,\mathrm{unp}} + (c^{\mathrm{BH}}_{1,\mathrm{unp}} + c^{\mathcal{I}}_{1,\mathrm{unp}} + \cdots)\cos\phi \cdot}$$

$$s_{1,\mathrm{LP}} \propto \Im\mathrm{m}\left[F_1\widetilde{\mathcal{H}} + \xi(F_1+F_2)\left(\mathcal{H} + \frac{x_B}{2}\mathcal{E}\right) + \right.$$
$$\left. - \xi\left(\frac{x_B}{2}F_1 + \frac{t}{4M^2}F_2\right)\widetilde{\mathcal{E}}\right].$$

$$A_{\mathrm{LL}}(\phi) \sim \frac{c^{\mathrm{BH}}_{0,\mathrm{LP}} + c^{\mathcal{I}}_{0,\mathrm{LP}} + (c^{\mathrm{BH}}_{1,\mathrm{LP}} + c^{\mathcal{I}}_{1,\mathrm{LP}})\cos\phi}{c^{\mathrm{BH}}_{0,\mathrm{unp}} + (c^{\mathrm{BH}}_{1,\mathrm{unp}} + c^{\mathcal{I}}_{1,\mathrm{unp}} + \cdots)\cos\phi \cdot}$$

$$c^{\mathcal{I}}_{0,\mathrm{LP}}, c^{\mathcal{I}}_{1,\mathrm{LP}} \propto \Re\mathrm{e}\left[F_1\widetilde{\mathcal{H}} + \xi(F_1+F_2)\left(\mathcal{H} + \frac{x_B}{2}\mathcal{E}\right) + \right.$$
$$\left. - \xi\left(\frac{x_B}{2}F_1 + \frac{t}{4M^2}F_2\right)\widetilde{\mathcal{E}}\right],$$

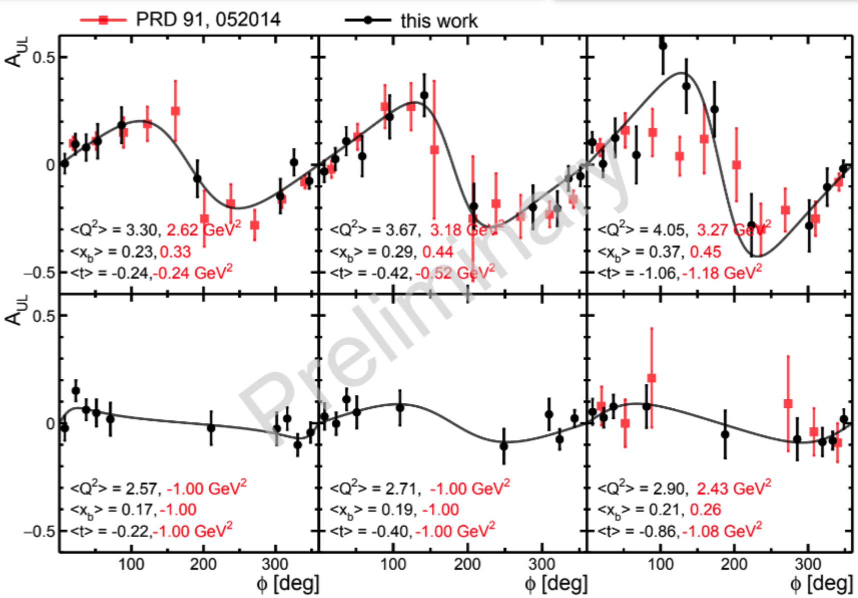

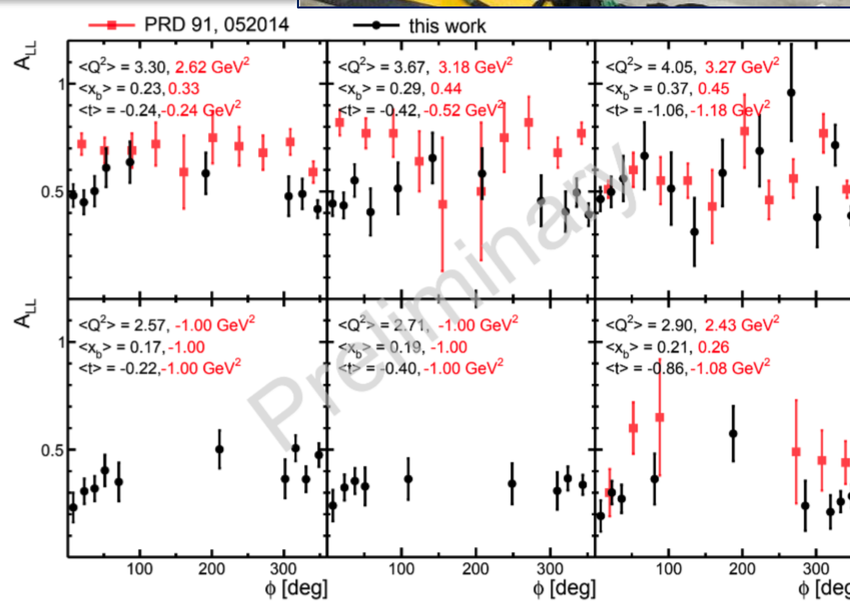

Nuclear DVCS: ALERT program

- Building on the successful CLAS experiment, which studied coherent and incoherent DVCS studies using a ^{4}He gaseous target,
- ALERT expands investigations of partonic structure of nuclei and nucleons over a broad kinematic range and multiple of final states, tagging recoil ^{4}He, ^{3}He, ^{3}H, and ^{2}H.
- Data taking is underway, and the ALERT detector is performing as expected.

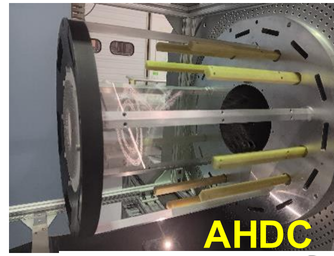

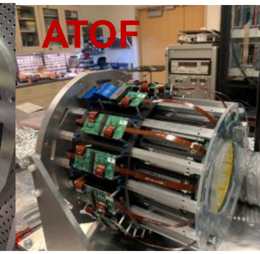

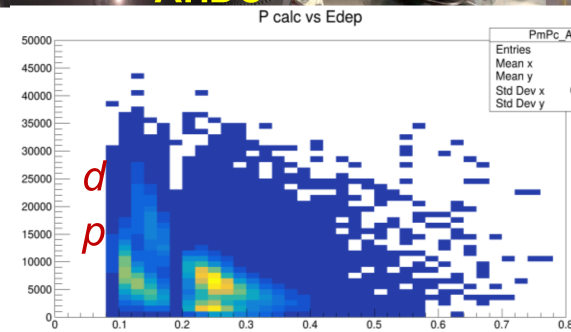

6 GeV CLAS results

$e^4He \rightarrow e'^4He'\gamma$

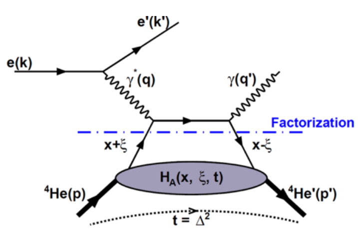

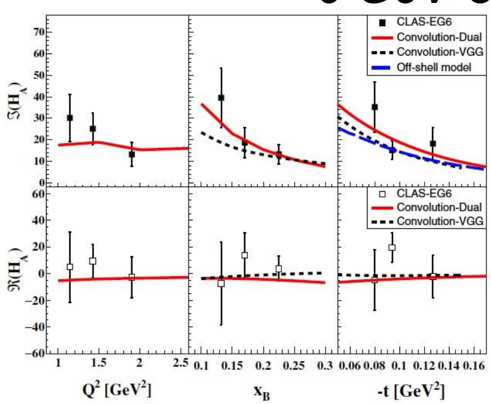

M. Hattawy *et al., Phys. Rev. Lett.* 119, 202004 (2017)

$e^4He \rightarrow e'p'\gamma X$

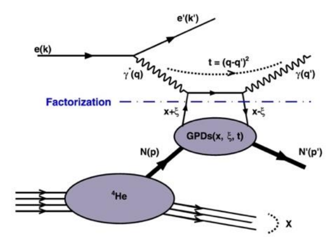

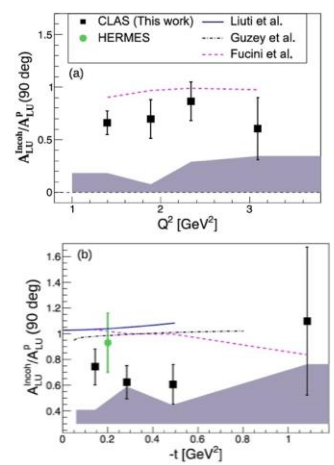

M. Hattawy *et al.,* Phys. Rev. Lett. 123, 032502 (2019)

DVCS with transversely polarized target

- A single target spin (UT) and double spin (LT) asymmetry give access to the imaginary and real parts of CFFs.
- The main target is CFF $\mathcal{E}$ (GPD E). Together with nDVCS, this experiment will provide data for flavor separation of GPD E.
- The experiment utilizes dynamically polarized NH3 situated inside HTCC, which requires a high magnetic field at the target. This necessitates a beam chicane and a new detector for DVCS protons.

$$A_{UT}^{\sin(\phi_S-\phi)} \propto \cos\phi\, \Im m(C_{TP}^{I}) \qquad A_{LT}^{\sin(\phi_S-\phi)} \propto \sin\phi\, \Re m(C_{TP}^{I})$$

$$C_{TP}^{I} \propto \frac{1-x_B}{2-x_B}\frac{t}{m^2}F_2\mathcal{H} + (2-x_B)\frac{t}{4m^2}F_1\mathcal{E}$$

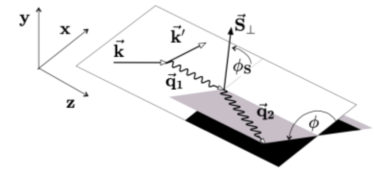

Projections

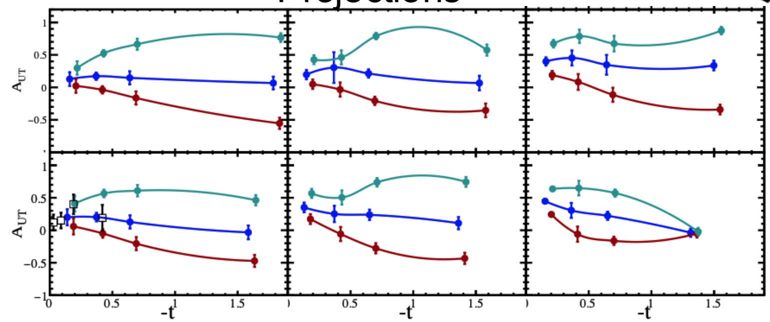

Target inside HTCC

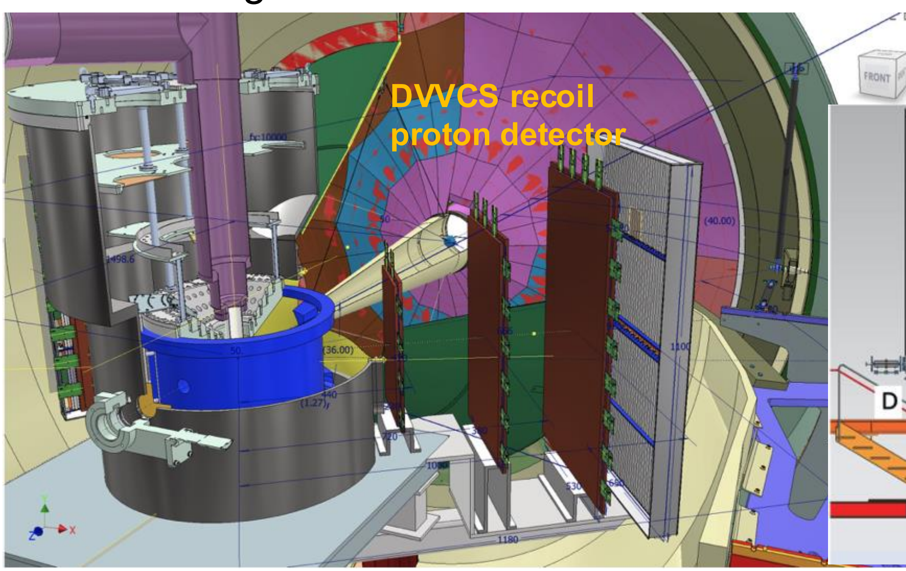

Beam chicane

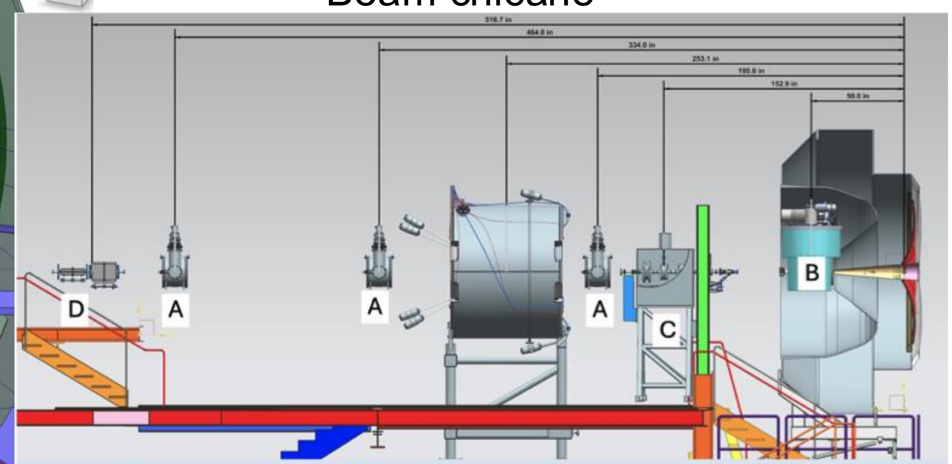

DVMP and transversity GPDs

A. Kim et al., CLAS collaboration, Phys. Lett. B 849 (2024) 138459.

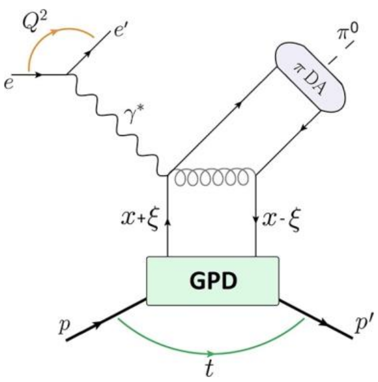

- Deeply virtual exclusive production of π^0 has an increased sensitivity to chiral-odd GPD, $\bar{E}_T = 2\widetilde{H}_T + E_T$.
- The $\sin\phi$ moment of BSA projects out $\sigma_{LT'}/\sigma_0$:

$$BSA = \frac{\sqrt{2\epsilon(1-\epsilon)}\frac{\sigma_{LT'}}{\sigma_0}\sin\phi}{1+\sqrt{2\epsilon(1+\epsilon)}\frac{\sigma_{LT}}{\sigma_0}\cos\phi+\epsilon\frac{\sigma_{TT}}{\sigma_0}\cos 2\phi}$$

$$\frac{\sigma_{LT'}}{\sigma_0} \sim \frac{Im[\langle\bar{E}_T\rangle^*\langle\widetilde{H}\rangle + \langle H_T\rangle^*\langle\widetilde{E}\rangle]}{(1-\xi^2)\left|\langle H_T\rangle\right|^2 - \frac{t'}{8m^2}\left|\langle\bar{E}_T\rangle\right|^2 + \epsilon\sigma_L}.$$

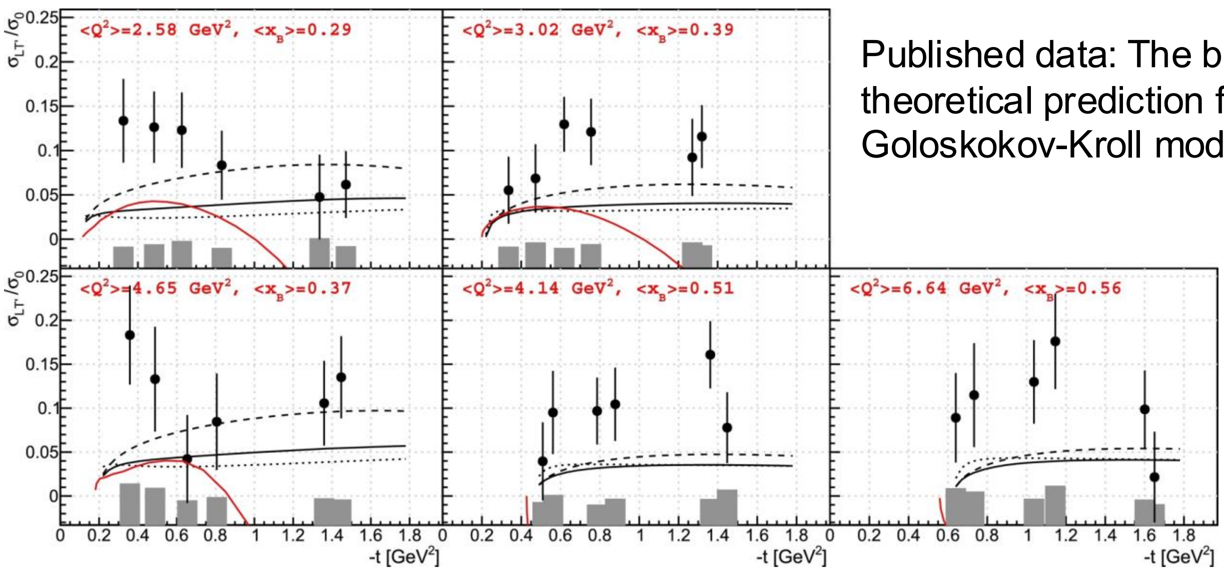

Published data: The black curves show the theoretical prediction from the GPD-based Goloskokov-Kroll model. The other curves are:

- The black dashed lines show the effect of the GPD $\tilde{E}_T$ multiplied by a factor of 0.5,
- the black dotted lines show the effect of the GPD $H_T$multiplied by a factor 0.5.
- The red curve shows the theoretical predictions from the Regge-based JML model.

First experimental measurement of TCS

Time-like Compton Scattering (TCS) mirrors DVCS in symmetry – a real incoming photon and an outgoing photon with substantial time-like virtuality (hard scale).

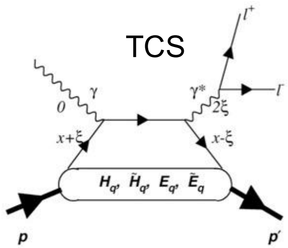

\+

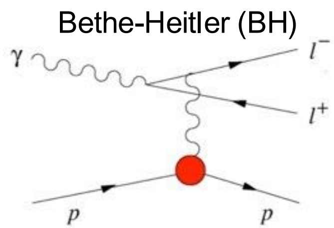

TCS is measured with the dominant BH process:

$$\sigma = \sigma_{BH} + \sigma_{INT} + \sigma_{TCS}$$

Unlike DVCS, the interference term provides access to both the real and imaginary parts of CFF in $\cos\varphi$ and $\sin\varphi$ modulations, respectively.

$$\frac{d\sigma_{INT}}{dQ'^2\,dt\,d(\cos\theta)\,d\varphi} = -\frac{\alpha_{em}^3}{4\pi s^2}\frac{1}{-t}\frac{M}{Q'}\frac{1}{\tau\sqrt{1-\tau}}\frac{L_0}{L}\left[\cos\varphi\frac{1+\cos^2\theta}{\sin\theta}\mathrm{Re}\tilde{M}^{--}\right.$$
$$\left.-\cos 2\varphi\sqrt{2}\cos\theta\,\mathrm{Re}\tilde{M}^{0-} + \cos 3\varphi\,\sin\theta\,\mathrm{Re}\tilde{M}^{+-} + O\left(\frac{1}{Q'}\right)\right]$$
$$-\lambda\frac{\alpha_{em}^3}{4\pi s^2}\frac{1}{-t}\frac{M}{Q'}\frac{1}{\tau\sqrt{1-\tau}}\frac{L_0}{L}\left[\sin\varphi\frac{1+\cos^2\theta}{\sin\theta}\mathrm{Im}\tilde{M}^{--}\right.$$
$$\left.-\sin 2\varphi\sqrt{2}\cos\theta\,\mathrm{Im}\tilde{M}^{0-} + \sin 3\varphi\,\sin\theta\,\mathrm{Im}\tilde{M}^{+-} + O\left(\frac{1}{Q'}\right)\right].$$

Photon polarization

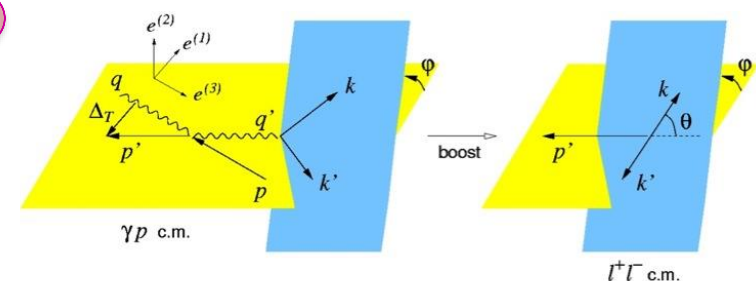

$$\tilde{M}^{--} = \frac{2\sqrt{t_0 - t}}{M}\frac{1-\xi}{1+\xi}\left[F_1(t)\mathcal{H} - \xi\big(F_1(t)+F_2(t)\big)\tilde{\mathcal{H}} - \frac{t}{4M^2}F_2(t)\mathcal{E}\right]$$

CLAS12 measures the reaction $ep \to l^+l^-p'(X)$, where the scattered electron is identified in the missing momentum analysis, $\mathrm{X} \equiv \mathrm{e}'$, with $P_\perp \approx 0$ (quasi-real photoproduction).

First experimental results

P. Chatagnon, et al., CLAS Collaboration, Phys. Rev. Lett. 127, 262501 (2021).

Two observables:

- Photon helicity asymmetry, accessing the imaginary part of the CFF (similar to BSA in DVCS) – testing the universality of GPDs:

$$A_{\odot U} = \frac{1}{P_b}\frac{N^+ - N^-}{N^+ + N^-} = \frac{d\sigma^+ - d\sigma^-}{d\sigma^+ + d\sigma^-} = \frac{-\frac{\alpha_{em}^3}{4\pi s^2}\frac{1}{-t}\frac{m_p}{Q'}\frac{1}{\tau\sqrt{1-\tau}}\frac{L_0}{L}\sin\phi\frac{(1+\cos^2\theta)}{\sin(\theta)}\mathrm{Im}\tilde{M}^{--}}{d\sigma_{BH}}$$

- Forward-backward asymmetry (exchange of e^+ and e^- momenta), accessing the real part of the CFF – extracting the *D*-term (QCD EMT FF $D^Q(t)$):

$$\mathbf{A_{FB}}(\theta_0,\phi_0) = \frac{\mathbf{d}\sigma(\theta_0,\phi_0) - \mathbf{d}\sigma(\pi-\theta_0,\pi+\phi_0)}{\mathbf{d}\sigma(\theta_0,\phi_0) + \mathbf{d}\sigma(\pi-\theta_0,\pi+\phi_0)} = \frac{-\frac{\alpha_{em}^3}{4\pi s^2}\frac{1}{-t}\frac{m_p}{Q'}\frac{1}{\tau\sqrt{1-\tau}}\frac{L_0}{L}\cos\phi_0\frac{(1+\cos^2\theta_0)}{\sin(\theta_0)}\mathrm{Re}\tilde{\mathbf{M}}^{--}}{\mathbf{d}\sigma_{BH}(\theta_0,\phi_0) + \mathbf{d}\sigma_{BH}(\pi-\theta_0,\pi+\phi_0)}$$

$\bar{E}_\gamma = 7.29\ GeV;\ \bar{M}_{ll} = 1.8\ GeV$

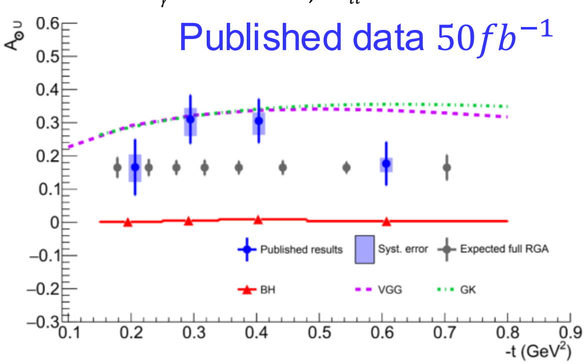

$\bar{E}_\gamma = 7.23\ GeV;\ \bar{M}_{ll} = 1.81\ GeV$

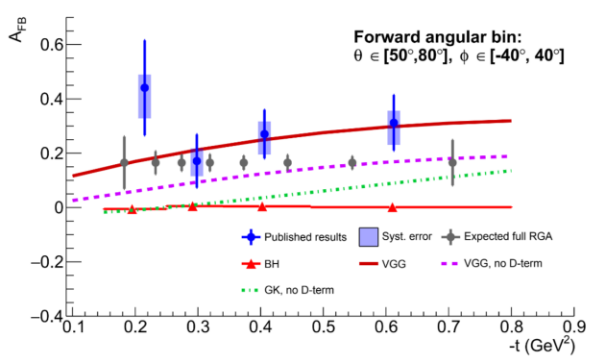

$\bar{E}_\gamma = 8.13\ GeV;\ \bar{M}_{ll} = 2.25\ GeV$

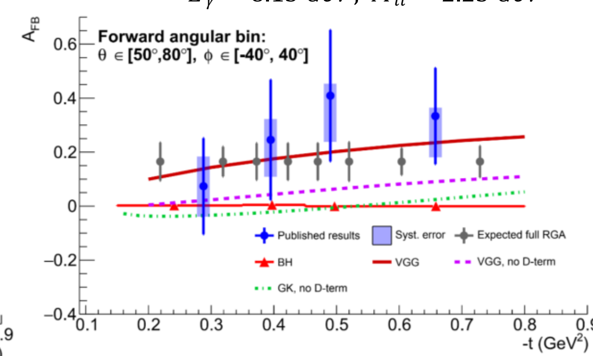

The currently available data for analysis is about $155fb^{-1}$. The expected full data set will be $760fb^{-1}$ (grey predictions on the plots).

Closing the loop on VCS

JLAB Flagship program – accessing GPDs through measurements of beam/target asymmetries and the cross sections of Compton processes (TCS and DVCS)

First experimental measurement with CLAS12 PRL 127, 262501 (2021)

TCS

Hard scale is defined by time-like photons

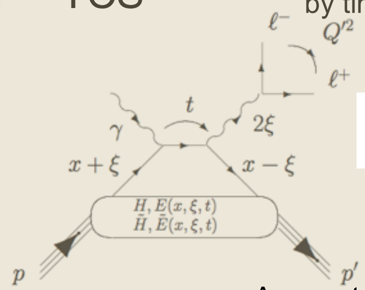

$$Re\ \mathcal{H}(\xi,t) = PV \int_{-1}^{1} dx\, C^{-}(\xi,x) H(x,\xi,t)$$

$$Im\ \mathcal{H}(\xi,t) = i\pi H(\xi,\xi,t)$$

Access to the Re-part of the Compton amplitude

Started in 2001, PRL 87, 182002. Now is the flagship physics program

DVCS

Hard scale is defined by space-like photon

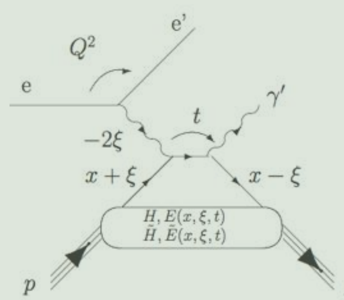

Jefferson Lab at the luminosity frontier is the only place in the world DDVCS can be measured!

μCLAS12 in Hall B and SoLID in Hall A are the two proposed facilities capable of carrying out such measurements.

DDVCS

Both space-like and time-like photons can set the hard scale

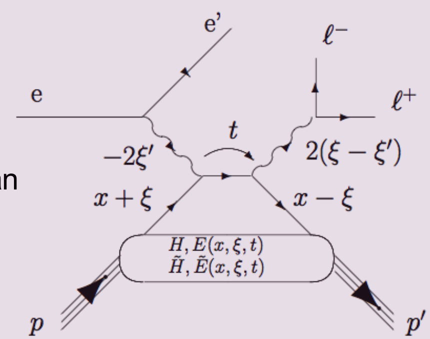

$$\int_{-1}^{+1} dx \frac{H(x,\xi,t)}{x-(2\xi'-\xi)+i\epsilon} + \ldots$$

$$H(2\xi'-\xi,\xi,t) + H(-(2\xi'-\xi),\xi,t)$$

σ-DDVCS is three orders of magnitude smaller than σ-DVCS

μCLAS12 for muon-electroproduction

Challenges in DDVCS measurements:

a) The cross-section is four orders of magnitude smaller than that of DVCS;

b) Ambiguities and anti-symmetrization issues with the decay leptons of the outgoing virtual photon and the incoming-scattered lepton.

Upgraded CLAS12 for:

$$ep \rightarrow e'p'\mu^+\mu^- \;\; @\, L > 10^{37} cm^{-2} sec^{-1}$$

Replace HTCC with wECal and Pb-shield, CD with trackers, and SC-pixel detector

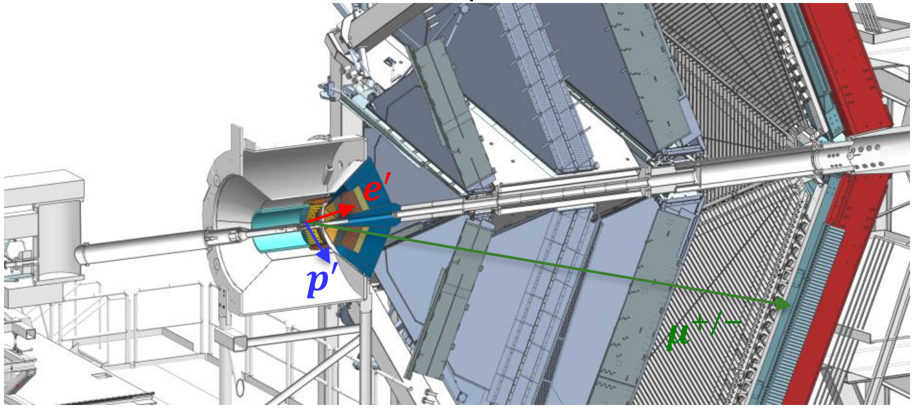

$$\xi = \frac{Q^2 + Q'^2}{2Q^2/x_B - Q^2 - Q'^2 + t}$$

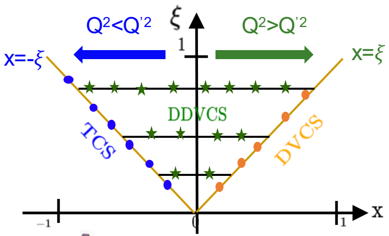

Spin asymmetries (Im, $x = \xi$) HERMES, CLAS, Hall A, JLAB12, COMPASS

Angular asymmetry in TCS (|Re|) JLAB12

Charge asymmetry in DVCS (|Re|) HERMES, COMPASS, JLAB12

DVCS Cross sections (|Re|²) H1, Hall A, JLAB12, COMPASS

DDVCS (Im, $x \neq \xi$)

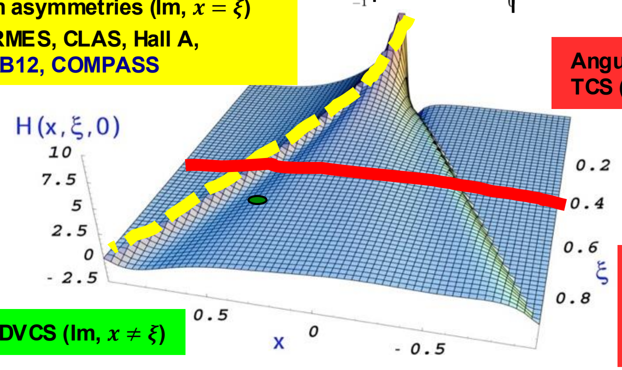

Kinematic coverage

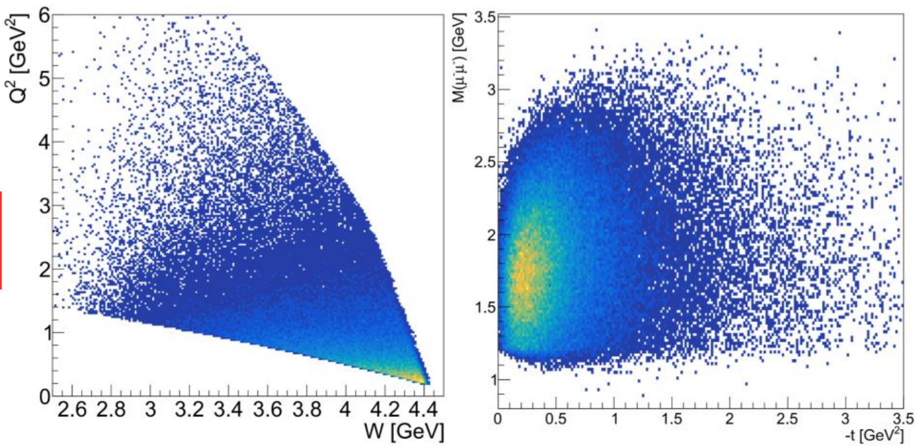

BSA in DDVCS

Key measurements include:

- A_{LU} in the transition from a **time-like** to a **space-like** region to validate the GPD formalism;
- *t*-dependence of A_{LU} to constrain models;
- Contribute to resolving the **shadow GPDs**.

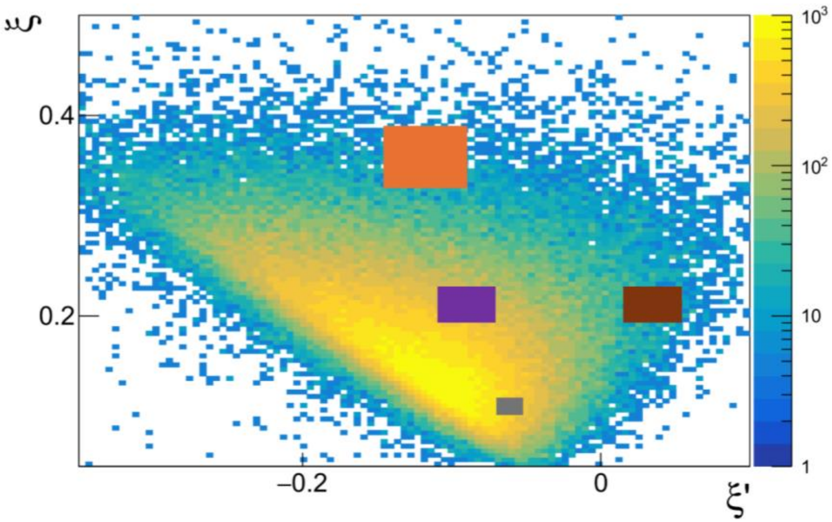

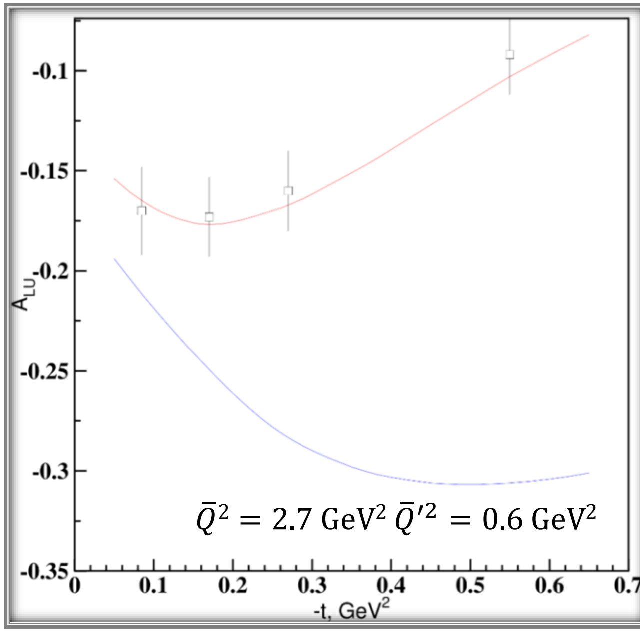

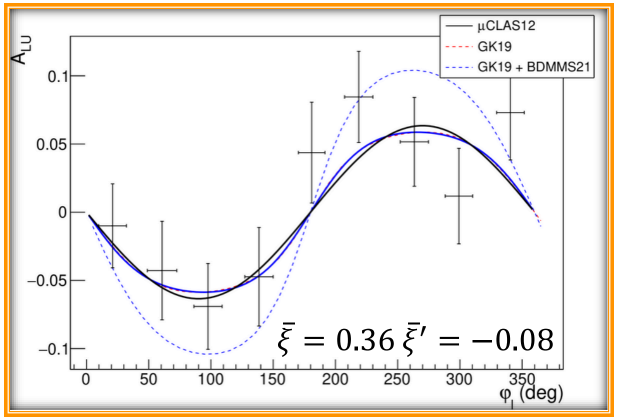

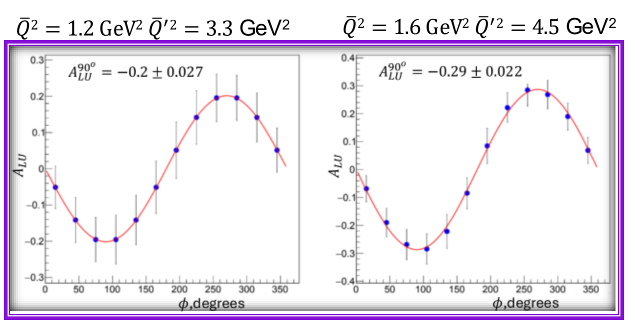

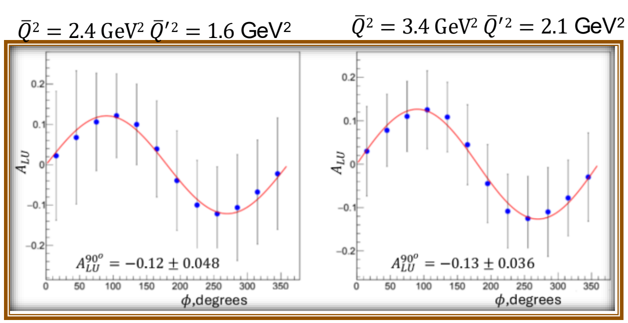

Near-threshold J/ψ photoproduction

- Several models connect the t-dependence of charmonium production near the energy threshold to the gluon gravitational form factor (GFF) of the proton.
- Unique access to the gluonic structure of the nucleon, to the mass and scalar radii, and the pressure distribution generated by the gluons.
- CLAS12 has comparable statistics to GlueX and J/ψ-007, and will publish the first results in the coming months.

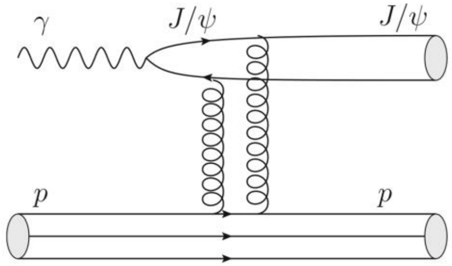

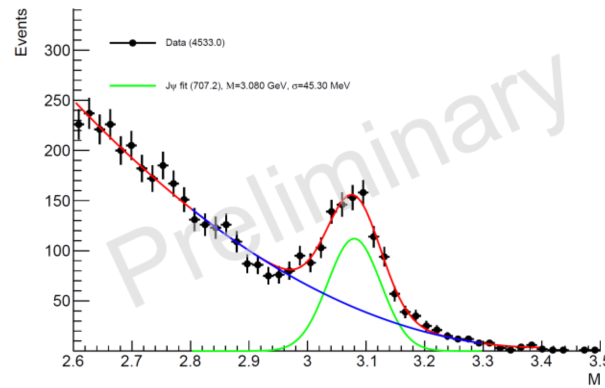

Total cross-section

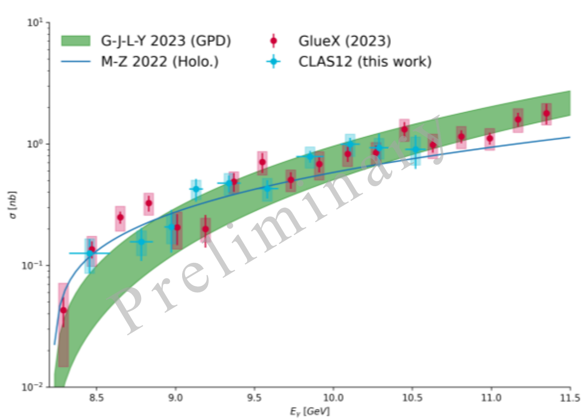

Dipole fits of the differential cross-section

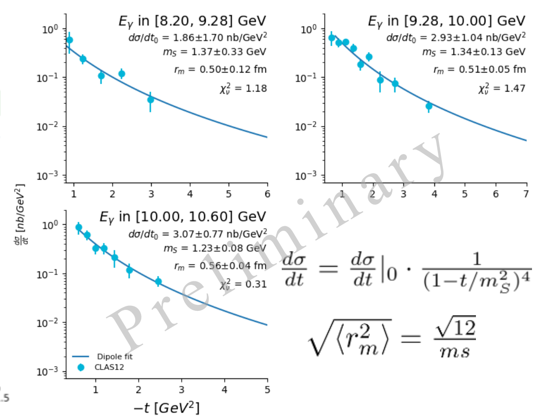

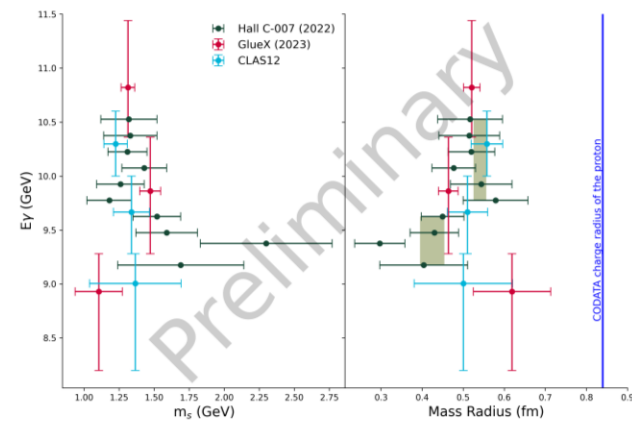

Summary

- The description of the partonic structure of hadronic matter is a major focus of JLAB's 12 GeV program.
- A comprehensive program to study GPDs using deeply virtual exclusive processes is underway in Hall B with the CLAS12 detector and up to 11 GeV polarized electron beams.
- The initial results have been released, featuring the first-ever measurement of TCS and DVCS BSA on the proton and neutron in new, unexplored kinematic regions, as well as BSA in deeply virtual p0 production.
- More results, including data from polarized targets, on nuclear DVCS and near-threshold charmonium production, will be available soon.
- These data are critically important yet limited for inferring information on GPDs from experimental observables.
- The collaboration is working on upgrading the luminosity to measure the Double DVCS process, which allows for the mapping of GPDs in x-space.